Analysis and optimization of an all-fiber device based on photonic crystal fiber with integrated electrodes

Giancarlo Chesini,[1] Valdir A. Serrão,[2] Marcos A. R. Franco,[2,3] and Cristiano M. B. Cordeiro,[1,*]

[1]*Instituto de Física "Gleb Wataghin", Universidade Estadual de Campinas, UNICAMP, Campinas, SP, Brazil*
[2]*Instituto de Estudos Avançados (IEAv), São José dos Campos, SP, Brazil*
[3]*Instituto Tecnológico de Aeronáutica (ITA), SP, Brazil*
**cmbc@ifi.unicamp.br*

Abstract: We present both numerical and experimental studies of an all-fiber device based on the integration of metallic electrodes into photonic crystal fibers (PCF). The device operation consists on applying electrical current to the electrodes which, by Joule effect, expand and squeeze the PCF microstructure in a preferential direction, altering both phase and group birefringence. We investigate the effect of integrating electrodes into the fiber and the dependence of the device sensitivity on the electrode configuration and composition.

OCIS codes: (060.2310) Fiber optics; (230.3990) Microstructure devices; (999.999) Photonic crystal fibers.

References and links

1. P. Russell, "Photonic crystal fibers," Science **299**(5605), 358–362 (2003).
2. M. Fokine, L. E. Nilsson, A. Claesson, D. Berlemont, L. Kjellberg, L. Krummenacher, and W. Margulis, "Integrated fiber Mach-Zehnder interferometer for electro-optic switching," Opt. Lett. **27**(18), 1643–1645 (2002).
3. H. Knape, and W. Margulis, "All-fiber polarization switch," Opt. Lett. **32**(6), 614–616 (2007).
4. Z. Yu, W. Margulis, O. Tarasenko, H. Knape, and P.-Y. Fonjallaz, "Nanosecond switching of fiber Bragg gratings," Opt. Express **15**(22), 14948–14953 (2007).
5. T. T. Larsen, A. Bjarklev, D. S. Hermann, and J. Broeng, "Optical devices based on liquid crystal photonic bandgap fibres," Opt. Express **11**(20), 2589–2596 (2003).
6. B. J. Eggleton, C. Kerbage, P. S. Westbrook, R. S. Windeler, and A. Hale, "Microstructured optical fiber devices," Opt. Express **9**(13), 698–713 (2001).
7. F. Beltrán-Mejía, G. Chesini, E. Silvestre, A. K. George, J. C. Knight, and C. M. B. Cordeiro, "Ultra-high birefringent squeezed lattice photonic crystal fiber with rotated elliptical air-hole," Opt. Lett. (to be published).
8. G. Chesini, C. M. B. Cordeiro, C. J. S. de Matos, M. Fokine, I. C. S. Carvalho, and J. C. Knight, "All-fiber devices based on photonic crystal fibers with integrated electrodes," Opt. Express **17**(3), 1660–1665 (2009).
9. J. Limpert, T. Schreiber, A. Liem, S. Nolte, H. Zellmer, T. Peschel, V. Guyenot, and A. Tünnermann, "Thermo-optical properties of air-clad photonic crystal fiber lasers in high power operation," Opt. Express **11**(22), 2982–2990 (2003).
10. S. H. Lee, B. H. Kim, and W.-T. Han, "Effect of filler metals on the temperature sensitivity of side-hole fiber," Opt. Express **17**(12), 9712–9717 (2009).
11. S. C. Rashleigh, "Wavelength dependence of birefringence in highly birefringent fibers," Opt. Lett. **7**(6), 294–296 (1982).

1. Introduction

Optical devices permit one to controllably change properties of light propagating through a medium. Fiber optical devices keep this feature and add the feasibility of straightforward integration into fiber based optical systems. Photonic Crystal Fibers [1] significantly extend possible configurations due the possibility of wide control of their opto-mechanical properties through the design of the air holes pattern.

#121557 - $15.00 USD Received 15 Dec 2009; revised 18 Jan 2010; accepted 19 Jan 2010; published 26 Jan 2010

In conventional fibers, used widely in telecom applications, light can be controlled through active or passive fiber optical devices, such as fiber amplifiers and Bragg grating based filters. To actively control light inside a fiber, a promising technique is to integrate electrodes into conventional-like fibers for purposes of electro optic switching [2–4]. In PCF's, on the other hand, the main approach is to insert electro-magneto-temperature sensitive materials inside the fiber (e.g. liquid crystals [5] or temperature dependent polymers [6]). Nonetheless, this approach does not explore the possibility of creating all-fiber devices. In this way, we fabricated a special kind of PCF with two external holes that can be used to squeeze the microstructure during fabrication, making ultra-high birefringent fibers [7] or, in a post-process step, be used to integrate electrodes [8]. Figure 1(a) shows a cross-sectional SEM image of this PCF with both external holes filled with a 43% Bi-57% Sn alloy electrodes. The alloy was inserted in the liquid state and then cooled down to room temperature [2–4, 8]. Devices made with these fibers can work applying electric field or electrical current in the electrode(s).

For polarization switching applications using electrical current [3, 8], the device operation consists, as shown schematically in Fig. 1(b), in applying an electrical current (*i*) to one electrode that heats by Joule effect. Heat is then dissipated to silica through conduction and, at the fiber-air interface, through convective flow. Temperature also causes the electrodes to expand inducing mechanical stress. These two effects depend linearly on the square of the electrical current since they come from power dissipation. Combined they change the effective refractive index felt by light. Thermo-optical phenomena were already studied in, e.g., high power fiber lasers [9]. Here, we present a numerical and experimental study of the thermo-mechanical-optical behavior of a PCF with integrated electrodes aiming the adjustment of its optical properties.

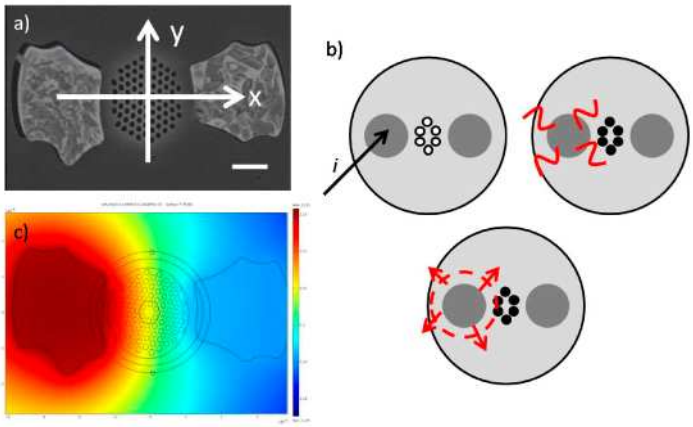

Fig. 1. (a) Cross-sectional SEM view of the PCF under study. White bar represents 10µm. (b) Schematic draw of the device operation. Electrical current is applied to one electrode that, by Joule effect, heats the entire fiber and squeezes the fiber microstructure. (c) Typical image of the temperature gradient inside the fiber after the application of electrical current. Red (blue) means higher (lower) temperature.

2. Numerical results

Temperature and thermally induced stress distributions can be simulated with finite elements methods [9]. In this work, simulations were carried out with a commercial software (COMSOL). All phenomena (electrical, thermal, mechanical and optical) were considered to be weakly coupled. In this way each problem is solved individually and the obtained physical parameters are used as input values to the following analysis. The parameters obtained directly from the simulations are temperature, stress, material refractive indices (N_x, N_y and N_z) and modal (neff-x and neff-y) effective indices of the fundamental modes. We calculate,

#121557 - $15.00 USD Received 15 Dec 2009; revised 18 Jan 2010; accepted 19 Jan 2010; published 26 Jan 2010

then, the material and phase modal birefringence, defined as $B_{mat}=N_y-N_x$ and $B_p=neff\text{-}_y–neff\text{-}_x$, respectively, with the x-direction being the one connecting both electrodes, Fig. 1(a). Three device configurations were studied: the one where both electrodes are active (two electrodes – Case I), the one where only one electrode is used (two electrodes, one active – Case II), and the one where there is only one electrode (i.e. the other big hole is not filled with metal – Case III).

The first parameter under study is temperature. Since silica dn/dT is $+1.2*10^{-5}$/°C the refractive index tends to increase with temperature. Figure 1(c) shows a typical image of the temperature gradient throughout the fiber after the application of electrical current in case II. Red (blue) represents higher (lower) temperature regions. Bi-Sn devices, e.g., have the core temperature increased by 2.5°C when 20mA current is applied for 500ms in cases II and III. When applying current to both electrodes simultaneously (case I), the enhancement is about twice this value. As for B_{mat}, initially, its value is zero, since silica is an isotropic material and hence $N_x = N_y = N_z$. As the electrical current is turned on, the metal heats, expands and squeezes the microstructure. B_{mat} is not affected by temperature since it changes both refractive indices equally. Compression, however, tends to squeeze the fiber core in the x-direction and to elongate it in the y-direction. This anisotropic compression causes the indices N_x, N_y and N_z to slightly differ, being the difference of the order of 10^{-5}. Regions of high stress (high $|B_{mat}|$) are observed around both electrodes.

The influence of thermal and mechanical effects makes light travelling through the fiber feel different effective refractive indices depending on the applied electrical current. In Fig. 2(a) we show the effective indices (neff-x and neff-y) for the orthogonal polarizations of the fundamental mode at 633nm. As can be seen, the indices are not equal at 0mA, which means the fiber is naturally birefringent. B_p at 0mA is calculated to be $4.1*10^{-5}$. Both refractive indices increase with electrical current, but at different rates. This can be explained by the fact that compression, as said before, is anisotropic, being neff-y more affected by it.

Figure 2(b) presents B_p for cases II and III. Although in both cases current is applied to only one electrode, and so the final temperature is the same, the presence of the second electrode, even when not being used, makes B_p more sensitive to electrical current. This indicates that the major influence on the modal effective indices is caused by stress, not temperature. Another interesting point to notice is that, since the derivative of B_p with respect to electrical current is not constant, the device efficiency can be adjusted by working within different ranges of electrical current. As an example, for the same Δi of 20mA in case II, Fig. 2(a), we calculated $B_{40mA}–B_{20mA}$ to be approx. 3.3 times higher than $B_{20mA}–B_{0mA}$ ($2.0*10^{-5}$ and $0.6*10^{-5}$, respectively), which amounts almost to the same difference between the squared electrical currents: $(40mA)^2-(20mA)^2 = 3 \times (20mA)^2-(0mA)^2$. This was expected since we're dealing with heat dissipation through Joule effect.

The results obtained in Fig. 2 (a) and (b) were calculated after 500ms of DC electrical current and give a good understanding on how the parameters change with current. In applications based on electro optic switching such as the one described in [8], however, one needs to simulate cycles of on-off electrical current. In Fig. 2(c) we present the case where a 20mA electrical current is turned on for 500ms, in case II, and then turned off for the same amount of time, repeatedly. As can be seen, after a few cycles the temperature enhancement (ΔT) stabilizes around 2.0°C for the bottom level and around 3.6°C for the upper level. Since temperature does not return to its initial value on the bottom level, ΔB_p calculated in this situation is expected to be smaller than that in Fig. 2(b). Indeed, ΔB_p for points 1 and 2 (ΔT=1.59°C) of Fig. 2(c) is $0.3*10^{-5}$ (half the value obtained in Fig. 2(b)). The birefringence-induced phase ($\Delta\varphi$) can then be calculated by Eq. (1) and, for the case of a L = 7cm device [8], is $\Delta\varphi \sim 0{,}67\pi$.

$$\Delta\varphi = \frac{2\pi}{\lambda}\cdot\Delta L \qquad (1)$$

#121557 - $15.00 USD Received 15 Dec 2009; revised 18 Jan 2010; accepted 19 Jan 2010; published 26 Jan 2010

It is instructive to realize that this 0-20mA on-off cycle is by no means a fixed quantity. As previously discussed, higher induced-birefringence can be achieved when working with higher electrical currents. We simulated then a 60-80mA on-off cycle (not shown) and obtained a $\Delta B_{60\text{-}80mA}$ of $3.0*10^{-5}$, which is ten times higher than $\Delta B_{0\text{-}20mA}$ - meaning a phase delay of approximately 6.7π.

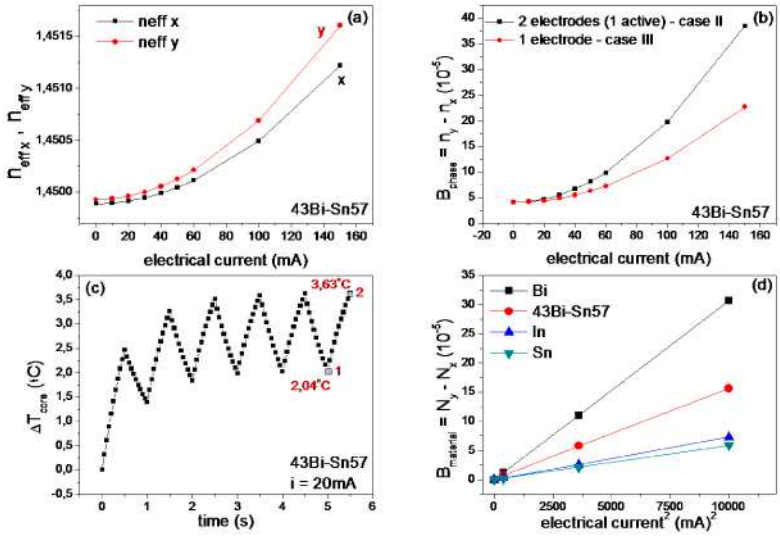

Fig. 2. (a) Effective refractive indices (neff-x and neff-y) of the fundamental mode at 633nm, as a function of the electrical current. (b) B_{phase} for two device configurations: two electrodes (one active) and one electrode (c) Temperature as a function of time for a 20mA on-off cycle. (d) Stress-induced material birefringence for different electrodes composition: Bismuth (Bi), 43Bi-Sn57 alloy, Indium (In), and Tin (Sn).

Besides the applied electrical current and the device configuration – one inactive, but present, electrode enhances the B change (Fig. 2(b), case II better than case III) - the device efficiency is also highly dependent on the electrode composition. This was already demonstrated in more conventional fibers but with the heat source external to them [10]. In that case the important parameter is the metal's thermal expansion coefficient. When the heat source is not external to the fiber but the electrode itself we have also to consider how it dissipates heat, meaning we have to look at its electrical conductivity. In Fig. 2(d) we present the induced material birefringence (B_{mat}) as a function of squared electrical current for bismuth (Bi), 43%Bi-57%Sn, tin (Sn) and indium (In) electrodes. While in [10] indium is the electrode that gives better sensitivity, it is readily observed that, in our case, this position is occupied by Bi electrodes. Even though In has the highest thermal expansion coefficient among the four metals ($\alpha_{In} = 32.1*10^{-6}$ K^{-1}, $\alpha_{Bi} = 13.2*10^{-6}$ K^{-1}) [10], Bi is a much poor electric conductor ($\sigma_{In} = 11.61*10^{+6}$ S/m, $\sigma_{Bi} = 0.87*10^{+6}$ S/m) [10], meaning, in our case, that Joule effect is enhanced in such samples. From here we can infer a recipe for devices based on heat dissipation and stress-induced-birefringence. Since the idea is to enhance Joule effect, the recipe depends whether you're working with a current source or a DC power supply. For the first case one needs a metal with low electric conductivity while for the second case it is necessary a high electric conductivity. In both cases high thermal expansion coefficient is required.

3. Experimental study

In order to verify what Fig. 2(d) states, devices made of Bi and 43%Bi-57%Sn electrodes were fabricated and put under the experimental setup presented in Fig. 3. The optical characterization consists on launching a linearly polarized He-Ne laser (633nm) through a

#121557 - $15.00 USD Received 15 Dec 2009; revised 18 Jan 2010; accepted 19 Jan 2010; published 26 Jan 2010

half-wave retarder (WP) making light enter the fiber at a 45° angle to both fiber polarization axes [8]. Light enters and leaves the fiber through objectives (O), heads towards a polarizer (P) and reaches a detector (D) connected to an oscilloscope (OSC). The polarizer was set to give the highest intensity through it.

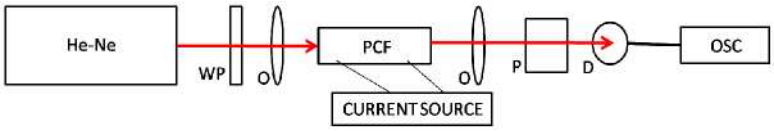

Fig. 3. Setup for optical characterization. A current source provides the electrical signal applied to the optical fiber.

Optical characterization consisted on applying an electrical current to the fiber for several seconds (to guarantee the device is stabilized) while following the optical signal on the oscilloscope. Figure 4 shows the measured intensities for (a) Bi-Sn electrodes and (b) Bi electrodes. The curves are vertically shifted to clarify the analysis. The black (lower) curves on both graphs show the electrical currents needed to throw the intensity into a minimum level and are 11mA and 9mA for Bi-Sn and Bi electrodes, respectively. The amplitude of this decay is determined by the ellipticity of light coming out of the fiber (77mm (Bi-Sn) and 60mm (Bi) long), which depends on its length (that was not optimized to give linear polarization). The phase differences between these two states (no current applied and minimum signal intensity) are defined as Φ_0(Bi-Sn) and Φ_0(Bi). From the point of minimum signal, to rotate the polarization by $\pi/2$ going from minimum to maximum (what gives a phase delay of π) we can see that 18mA are necessary in the Bi-Sn electrodes while to do the same in the Bi electrode only 14mA is required. To achieve a 2π delay in the Bi device it was necessary to apply 17mA while 20mA in the Bi-Sn device was not able to produce the same effect.

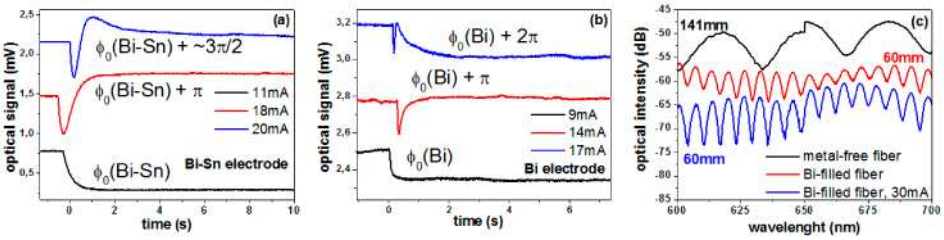

Fig. 4. Optical signal of (a) Bi-Sn and (b) Bi electrodes with the application of electrical current. Φ_0(Bi-Sn) and Φ_0(Bi) are the "intrinsic" phase related to the length of the device. Bi-Sn device requires 18mA to alter the phase of light by π while in the Bi device it takes only 14mA to do the same. (c) Pattern of a PCF without metal (black upper curve), with Bi electrodes (red middle curve) and with 30mA (blue lower curve) in the wavelength scanning method.

The absolute value of the electrical current is, because of Φ_0 and the need to go from elliptical to linear polarization, of low importance. In this way, to calculate $\Delta\Phi$ by Eq. (1) we considered the difference (ΔB) from each level to the reference (minimum) level. For instance, in the Bi-Sn device, between 11mA and 18mA levels $\Delta\Phi$ changes π-rad (Fig. 4(a)). From the simulation one can calculate ΔB between these two levels and, using this value in Eq. (1), to get 1.28π radians. From 11mA to 20mA the simulated $\Delta\Phi$ is 1.83π rad. For the Bi device (Fig. 4(b)), from 9mA to 14mA results in $\Delta\Phi$ of 1.04π while from 9mA to 17mA gives $\Delta\Phi = 1.68\pi$ rad.

Table 1 summarizes these results comparing the simulated and measured values for the current-induced birefringence (B), ΔB and $\Delta\Phi$ for each current of Fig. 4 (a) and (b). As we

#121557 - $15.00 USD Received 15 Dec 2009; revised 18 Jan 2010; accepted 19 Jan 2010; published 26 Jan 2010

can see, the estimated values for the phase delay differ less than 30% from the simulated and, as expected from Fig. 2(d), Bi devices are more efficient.

Table 1. Numerical results for 43Bi-Sn57 and Bi devices

43Bi-Sn57 electrodes					Bi electrodes				
***i* (mA)**	***B* (10^{-5})**	***ΔB* (10^{-5})**	***ΔΦ***	***ΔΦ exp.***	***i* (mA)**	***B* (10^{-5})**	***ΔB* (10^{-5})**	***ΔΦ***	***ΔΦ exp.***
11	*4.6*	*0*	Φ_0*(Bi-Sn)*	--	*9*	*4.7*	*0*	Φ_0*(Bi)*	--
18	*5.3*	*0.7*	1.28π	π	*14*	*5.5*	*0.8*	1.04π	π
20	*5.6*	*1.0*	1.83π	$\sim 3\pi/2$	*17*	*6.0*	*1.3*	1.68π	2π

The results of the relative phase birefringence (ΔB) presented so far allow determining the influence of applying electrical current to the device. To study and quantify the influence of the electrode integration (when comparing the same fiber with no electrode) absolute measurements of the group modal birefringence (B_g) were carried out using the wavelength scanning method [11] for fibers with 43Bi-Sn57 and Bi electrodes.

Figure 4(c) shows the measurements done in a 141 mm long fiber without metal (black upper curve), and in a 60mm PCF with integrated Bi electrodes but in the absence of electrical current (red middle curve) and with 30mA applied in the "two electrodes (one active) – case II" configuration (blue lower curve). The longer length of the PCF without metal is just to help the observation of the peak pattern. This was necessary due to the inversely proportional relation between $B_g(\lambda)$ and $\Delta\lambda$ (the distance between two adjacent peaks): $|B_g| = \lambda^2/(L\cdot\Delta\lambda)$, where L is the fiber lenght. The experimental results indicate that the insertion of the electrodes increases the original fiber birefringence, from $|B_g|=8.7*10^{-5}$ to $58*10^{-5}$ (Bi-Sn) and to $108*10^{-5}$ (Bi). We believe that this enhancement is due to the fact that filling the fiber with molten metal, and working with it in solid state, induces stress. Applying 30mA reduces $|B_g|$ from $58.1*10^{-5}$ to $57.1*10^{-5}$ (Bi-Sn) and from $108*10^{-5}$ to $96.2*10^{-5}$ (Bi).

Modeling such situation gives the same qualitative results: residual stress due the metal filling increase the original form $|B_g|$ and applying current reduces $|B_g|$. A good (quantitative) agreement was also obtained for the fiber without electrodes: $|B_g| = 8.7*10^{-5}$ (as stated above for the experimental value) and $|B_g|= 8.56*10^{-5}$ (modeling).

The modal group birefringence was determined by calculating $B_p(\lambda)$ around the wavelength of interest and using Eq. (2) [7].

$$B_g(\lambda) = B_p(\lambda) - \lambda\partial B_p(\lambda)/\partial\lambda \qquad (2)$$

4. Conclusions

Photonic crystal fibers give the possibility of creating monolithic devices. Here, we studied, both experimentally and numerically, a PCF with two integrated electrodes. The device operation is based on induced birefringence caused by mechanical stress when electrical current heats an internal electrode. In order to optimize its operation and to increase its sensitivity, different electrodes configurations and material were studied, as well as its response with the applied current. Bismuth electrodes have shown to be a good option due its large thermal expansion coefficient and (when using a current source) low electric conductivity. Experimental measurements confirm that analysis and the values of the modal phase birefringence agreed well with the simulated ones. A stress birefringence (without current applied) due the metal filling process was quantized via group birefringence measurements and simulations.

#121557 - $15.00 USD Received 15 Dec 2009; revised 18 Jan 2010; accepted 19 Jan 2010; published 26 Jan 2010

Acknowledgments

The authors thank CNPq/FAPESP (INCT program) and CAPES and CAPES) for the financial support, Soft Metais Ltda company for providing the alloys and metals and José Aparecido for his technical help.

#121557 - $15.00 USD Received 15 Dec 2009; revised 18 Jan 2010; accepted 19 Jan 2010; published 26 Jan 2010